

Article

Computational Fluid Dynamics Model for Analysis of the Turbulent Limits of Hydrogen Combustion

Ivan Yakovenko , Alexey Kiverin  and Ksenia Melnikova Joint Institute for High Temperatures of Russian Academy of Sciences, Izhorskaya St. 13 Bd. 2,
125412 Moscow, Russia

* Correspondence: yakovenko.ivan@bk.ru (I.Y.); alexeykiverin@gmail.com (A.K.)

Abstract: This paper presents a novel numerical approach for assessing the turbulent limits of hydrogen combustion. In the framework of this approach, the premixed combustion is studied numerically in the externally generated turbulent field with defined parameters. Two-dimensional calculations are carried out for hydrogen–air mixtures of different compositions, and all the possible modes of near-limit combustion are reproduced. Among these modes are: combustion in the form of spatially separated individual kernels and combustion in the form of kernels with subsequent quenching. The critical conditions between the mentioned two modes correspond to the turbulent limits of hydrogen combustion, which are necessary for the evaluation of the hazardous risks related to hydrogen explosions.

Keywords: turbulent combustion; flammability limits; hydrogen combustion; hydrogen safety; numerical analysis



Citation: Yakovenko, I.; Kiverin, A.; Melnikova, K. Computational Fluid Dynamics Model for Analysis of the Turbulent Limits of Hydrogen Combustion. *Fluids* **2022**, *7*, 343. <https://doi.org/10.3390/fluids7110343>

Academic Editors: Jian Fang and Mehrdad Massoudi

Received: 13 September 2022

Accepted: 29 October 2022

Published: 1 November 2022

Publisher's Note: MDPI stays neutral with regard to jurisdictional claims in published maps and institutional affiliations.



Copyright: © 2022 by the authors. Licensee MDPI, Basel, Switzerland. This article is an open access article distributed under the terms and conditions of the Creative Commons Attribution (CC BY) license (<https://creativecommons.org/licenses/by/4.0/>).

1. Introduction

Today, hydrogen energy is of great research interest, among other concepts of green energy. Hydrogen is one of the most hazardous gaseous fuels due to its wide flammability limits [1] and low ignition energy [2]. That is why the development of hydrogen energy is closely related to the issues of hydrogen safety, the risk assessment of hydrogen explosion, and the elaboration of measures for its mitigation. Hydrogen safety is also widely studied in the context of severe accidents at nuclear plants [3]. Scenarios of those accidents are associated with the accumulation of large amounts of hydrogen, which can be exploded after mixing with air. Moreover, there is a natural stratification of hydrogen, and the composition of the hydrogen–air mixture can vary in different areas of the reactor building. The same is true for the scenarios of accidental hydrogen release from storage systems [4,5]. So, evaluation of the concentration limits of different combustion modes can enable the reliable quantitative assessment of possible hazardous scenarios.

Via conventional experimental tools [6,7], one can estimate the critical conditions of the formation and propagation of a stable combustion wave in a premixed mixture after localized ignition. Thus, the lower concentration limit of hydrogen combustion (lean flammability limit) under normal conditions and terrestrial gravity is known to be in the range of 4% [1] to 6% of hydrogen [8]. However, the stable deflagration wave can be formed only in mixtures containing more than ~8–10% [9], while in the range from 4–6% to 8–10%, the combustion proceeds in the form of combustion kernels (flame balls or caps) rising upwards under the action of buoyancy force [10]. In those “ultra-lean” compositions, one can observe the flame propagation only upwards, and no combustion propagation is observed if the mixture is ignited at the top wall of the vessel. As shown recently in [11,12], the basic mechanism of combustion quenching in ultra-lean mixtures is related to the stretch of the initial burning kernel by the convective flow arising in the process of the kernel’s buoyant motion. As a result of stretching, the burning kernel breaks into smaller ones, which cannot sustain an exothermic reaction due to the larger relative effect of losses.

The same mechanism of flame quenching can be observed in a highly turbulent medium. In that case, the flame is stretched under the action of intense pulsations, breaking the flame front [13]. The continuity loss of the flame front results in the formation of separated unstable burning kernels. That leads to local or total quenching of the combustion [14]. Due to that mechanism, intense turbulence can quench the flame even in mixtures far from the concentration limits estimated in quiescent conditions [15,16]. The effect of the described scenario of turbulent flame quenching on the combustion limits has not been studied thoroughly [17].

Recently, numerous works have been devoted to the development of models of turbulent combustion [18]. While direct numerical simulation (DNS) can provide useful insights into the peculiarities of turbulent combustion, it is still out of reach to perform direct simulations of this process on industrial scales [19]. However, DNS is highly suitable as a reliable basis for the development and validation of simplified models appropriate to describe one or another turbulent combustion mode [20]. One of the crucial concepts in turbulent combustion is flame displacement speed, which is the speed with which a point on a flame surface moves along the local normal of the flame surface relative to the local fluid velocity. Many turbulent combustion models, such as models based on level-set equations [21] or flame surface density formalism [22], require a robust way to obtain flame displacement speed for relevant combustion conditions. One of the methods for flame displacement speed evaluation is based on the relation between flame displacement speed and the flame stretch quantified by Markstein length, provided by asymptotic theory [23]. A thorough examination of this approach, performed in [24], has shown that the displacement speed of a weakly-stretched flame depends only on two parameters—the stretch and curvature of the flame surface, with the associated separate Markstein lengths, and the good agreement between asymptotic theory and numerical simulation can be achieved if a proper isotherm is chosen for the evaluation of the flame displacement speed. Later in [25], this two-parameter Markstein length model was successfully implemented for the description of premixed turbulent combustion and verified against the DNS data on turbulent flame displacement speed. In the context of flame surface density methods, problems related to the prediction of convection fluxes are of particular importance (see, e.g., [26]). Another promising technique is employing a statistical description of the flow via evolution equations for probability density functions [27,28]. The probability density function method is a well-established field in numerical modeling and has received significant attention in recent decades [29]. However there is still room for improvement from both the conceptual and applied points of view. Thus, in a recent paper [30], new joint/inverse modeling strategies in the PDF method were introduced that allow the closed-form description of the combustion characterized by fast chemical reactions, while in [31] a new framework for flame front propagation in a turbulent medium at low Damköhler number was developed, which expands the applicability of the PDF approach to the regimes with thick preheat zones.

Despite the wide research interest in the problems of turbulent combustion, the issues related to the turbulent combustion limits have not been fully understood. There is no such comprehensive research and application of the different modeling approaches mentioned above for near-limit flames, and only a few papers employing numerical modeling to address this issue can be mentioned here [32,33]. In [33], a direct numerical simulation was performed to investigate the conditions for turbulent quenching of the flame kernel in rich ($\phi = 4$) hydrogen–air mixtures at different values of the root mean square turbulent velocity u_{rms} . In [32], the authors proposed the problem setup for studying flame extinction in turbulent flows and employed this approach to obtain a lean turbulent combustion limit in hydrogen–air mixtures.

This paper is devoted to the formulation of a numerical model of the turbulent combustion of hydrogen–air mixtures for analysis of the turbulent combustion limits in lean mixtures. The proposed model is applied to estimate the turbulent combustion limit for lean and ultra-lean hydrogen–air mixtures on the base of a two-dimensional problem setup. The approach for the analysis of turbulent combustion limits is demonstrated in the case of

the obtained numerical results. Further, the proposed model can be applied for full-scale three-dimensional calculations, and better assessments can be achieved for the applied problems of lean turbulent combustion of hydrogen-based mixtures.

2. Problem Setup

When simulating the combustion of gaseous mixtures of real compositions numerically, it is necessary to resolve a local structure of the flame front, which is of the order of 1 mm in the case of lean hydrogen–air mixtures. That is the main difficulty of the direct numerical simulation of combustion. Moreover, one should take into account the detailed kinetics of combustion to reproduce the various chemical features of combustion accurately, including the phenomenon of flame quenching. Both mentioned factors severely restrict the opportunities for direct numerical simulations due to limited computational resources. Consequently, one can carry out three-dimensional calculations only for rather small-scale vessels, and currently, two-dimensional calculations are the main tool to study in detail the non-steady development of the flame front, including its propagation, interaction with the flow, and quenching. At the same time, however, the recent experience in the comparison between the experimental and numerical data on lean hydrogen–air combustion [34] shows that even two-dimensional calculations reproduce the experimentally observed features with sufficiently good accuracy. As well, the two-dimensional calculations presented in [12,35] agreed quite well with the experimental data on the combustion limits under terrestrial [1,8] and microgravity [36] conditions. Given the similarity of the quenching mechanism reported in [11] and the one responsible for turbulent flame quenching, one can assume that even two-dimensional calculations would provide more or less accurate quantitative characteristics of flame quenching under the action of turbulence, at least in the case of lean hydrogen–air mixtures.

The governing equations represent the full Navier–Stokes model with an account of the thermal conductivity, multicomponent diffusion, and energy release associated with the chemical transformations [37]. Due to the low intensity of the process of near-limit combustion, it is reasonable to utilize low-Mach approximation to avoid the strict limitations on the time step of numerical integration [38]. The mathematical model used here is presented below and can be found in detail in [39].

$$\frac{\partial \rho}{\partial t} + \frac{\partial \rho u_i}{\partial x_i} = 0 \tag{1}$$

$$\frac{\partial \rho Y_k}{\partial t} + \frac{\partial \rho Y_k u_i}{\partial x_i} = \nabla \rho Y_k V_{k,i} + \dot{\omega}_k \tag{2}$$

$$\frac{\partial \vec{u}}{\partial t} - \vec{u} \times \vec{\omega} + \nabla H - \bar{p} \nabla \left(\frac{1}{\rho} \right) = \frac{1}{\rho} \left[\nabla \cdot \sigma + \vec{f}(\vec{x}, t) \right] \tag{3}$$

$$\begin{aligned} \frac{\partial \rho h_s}{\partial t} + \frac{\partial \rho h_s u_i}{\partial x_i} &= \frac{d\bar{p}}{dt} - \sum_{k=1}^N \dot{\omega}_k \Delta h_{f,k}^0 \\ - \frac{\partial}{\partial x_i} \left(\rho \sum_{k=1}^N h_{s,k} Y_k V_{k,i} \right) &- \frac{\partial}{\partial x_i} \left(\kappa \frac{\partial T}{\partial x_i} \right) + \sigma_{ij} \frac{\partial u_i}{\partial x_j} \end{aligned} \tag{4}$$

$$\sigma_{ij} = \mu(Y_k, T) \left[\frac{\partial u_i}{\partial x_j} + \frac{\partial u_j}{\partial x_i} - \frac{2}{3} \delta_{ij} \frac{\partial u_l}{\partial x_l} \right] \tag{5}$$

$$\bar{p} = \rho RT \sum_k \frac{Y_k}{M_k} \tag{6}$$

$$dh_s = C_p(Y_k, T) dT \tag{7}$$

Here, ρ is the mass density, \vec{u} is the mass velocity, u_i are the mass velocity vector components, Y_k is the mass fraction of the k -th component of the gaseous mixture, M_k

is the molecular weight of the k -th component of the gaseous mixture, \tilde{p} is the dynamic component of the pressure fluctuations, which is by the order of magnitude much smaller compared with the thermodynamic pressure \bar{p} and $p(\vec{x}, t) = \bar{p}(t) + \tilde{p}(\vec{x}, t)$, σ is the viscous stress tensor, σ_{ij} are the components of the viscous stresses tensor, $H = |\vec{u}^2|/2 + \tilde{p}/\rho$ is the stagnation energy per unit mass, $\vec{\omega}$ is the vorticity vector, h_s is the specific sensible enthalpy of the mixture, $h_{s,k}$ is the specific sensible enthalpy of the k -th component of the gaseous mixture, T is the temperature, $\kappa(Y_k, T)$ is the thermal conductivity coefficient, $\mu(Y_k, T)$ is the viscosity coefficient, $h_{f,k}^0$ is the enthalpy of formation of the k -th component of the gaseous mixture, $\vec{V}_{k,i}$ is the diffusion velocity vector component of the k -th specie, and $C_p(Y_k, T)$ is the specific heat capacity at the constant pressure of the mixture. Term $\dot{\omega}_k$ represents the change in mass fraction of the k -th specie due to the chemical reactions.

When calculating the equation of state of the multicomponent mixture (7), the data from [40] were used. The diffusion was modeled in the zeroth-order Hirshfelder–Curtiss approximation [41]. Mixture averaged transport coefficients were obtained from the gas kinetics theory [42]. The correction velocity approach proposed in [43] was used to calculate the diffusion velocities. The chemical kinetics of hydrogen oxidation were modeled according to the detailed kinetic mechanism from [44].

The governing equations were solved with the second-order predictor/corrector method described in [45]. The computational cell size was chosen based on the specific convergence tests carried out for each mixture composition and aimed at the definition of the flame thickness. It was shown that using computational cells of 0.1 mm linear size was enough to resolve the flame thickness in the 10% hydrogen–air mixture with only 0.19% error relative to the limit value obtained by the conventional Richardson extrapolation routine (Figure 1a). In Figure 1b, the characteristic dependence of the flame front thickness on the hydrogen content in a mixture with air is presented for the computational cell $\Delta x = 0.1$ mm. One can see that the flame thickness increased with the decrease in the hydrogen content; so, the chosen resolution was enough for lean mixtures.

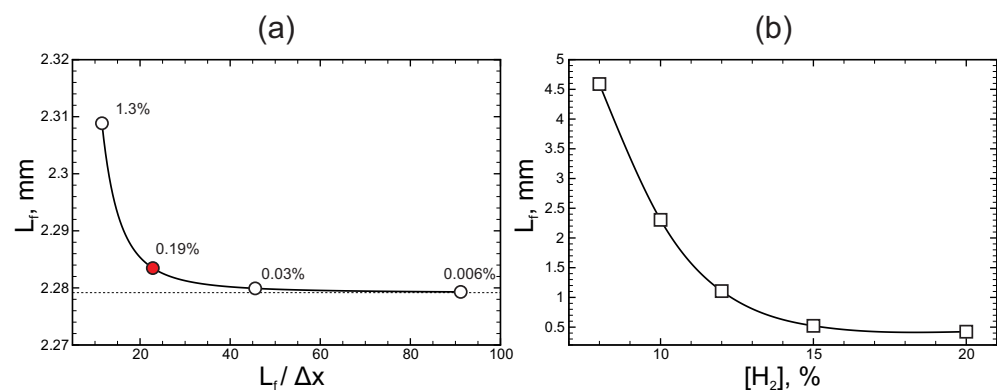


Figure 1. (a) Convergence test: dependence of the flame thickness in 10% hydrogen–air mixture on the grid resolution. (b) Dependence of the flame thickness on the hydrogen content in the mixture with air ($\Delta x = 0.1$ mm).

We propose to use the concept of the synthetic generation of homogeneous isotropic turbulence, which represents a stationary process by itself, to model turbulent combustion. Such a concept is widely used in the literature [46–48], and in particular, in [49], it was shown that the application of this concept in two-dimensional calculations provided quite good agreement with the three-dimensional experiments. So, even knowing that the characteristics of synthetic homogeneous isotropic turbulence in two- and three-dimensional cases are different, one can use a two-dimensional problem setup as a first approximation. To generate the stationary turbulence, let us introduce the following source to the momentum Equation (3) [50]:

$$\vec{f}(\vec{x}, t) = \frac{\kappa}{\sqrt{\tau}} \cdot \text{Re} \left(\frac{\vec{k} \times \vec{e}}{\sqrt{k^2 - (\vec{k} \cdot \vec{e})^2}} \exp(i\vec{k}\vec{x} + i\phi(t)) \right); \quad (8)$$

here, \vec{u} —velocity vector, t —time, \vec{x} —coordinate vector, \vec{f} —source term responsible for turbulence generation, κ —magnitude of the perturbation, τ —time step of calculation, \vec{k} —spatial frequency corresponding to the forcing scale λ_f , $|\vec{k}| = 2\pi/\lambda_f$, the direction of \vec{k} is randomized at each time step, \vec{e} —unity vector, and $\phi(t)$ —random phase.

The combustion process is considered inside a two-dimensional domain with open boundaries (Figure 2a) that mimic the combustion in the unconfined space. The space is filled with a hydrogen–air mixture of a given composition at normal conditions ($T_0 = 300$ K, $p_0 = 1$ atm). Firstly, the homogeneous isotropic turbulence was generated in the fresh mixture according to Equations (1) and (2) with $\lambda_f = 5$ mm, which corresponds to the estimation of the Euler scale of turbulence in [51] (Figure 2b). After a stationary solution was achieved (Figure 2c), the ignition was initiated in the central part of the domain (Figure 2a). Such a problem setup was close to the experimental conditions [52], where the combustion at the background of the homogeneous isotropic turbulence was studied.

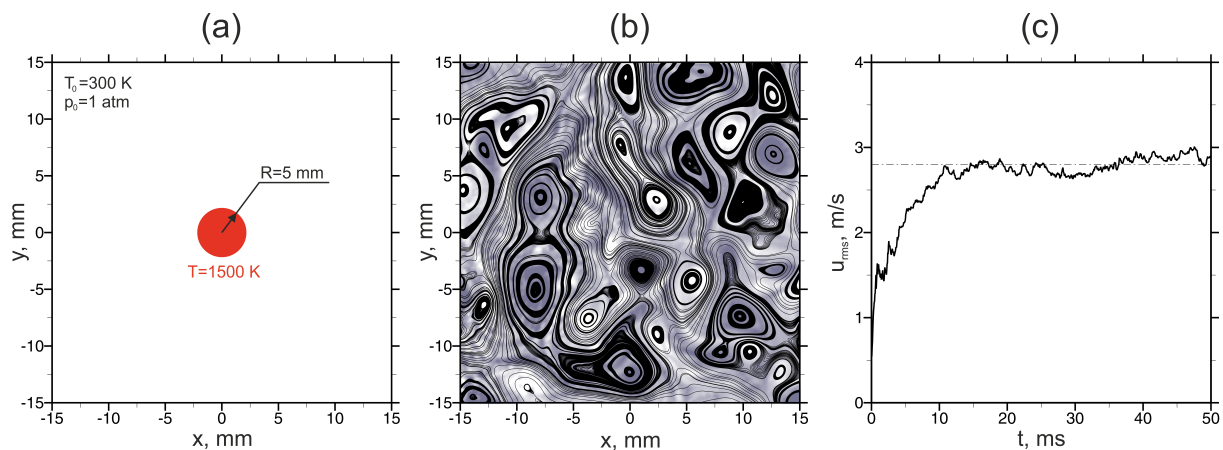


Figure 2. (a) Schematic of the problem setup. (b) Stream traces at the background of the normalized vorticity field illustrating the homogeneous isotropic two-dimensional turbulence generated via Equations (1) and (2) with $\lambda_f = 5$ mm. (c) Time dependence of the root mean square velocity characterizing the development of the synthetic turbulence.

Although here we mainly discuss a numerical approach for the estimation of lean turbulent limits and mechanisms of the flame quenching under the influence of turbulence, possible uncertainties in the prediction of the lean turbulent limits should be highlighted. First of all, the major source of uncertainty is related to the step of varying the u_{rms} value. Thus, for the mixture with 8% hydrogen content, the stable combustion was observed in turbulent flow with a u_{rms} equal to 3.8 m/s, while for $u_{rms} = 4.35$ m/s, the quenching of the flame occurred. Thereby, the possible error reached ± 0.5 m/s or about 10% relative error. Similar estimations are valid for other mixture compositions. The second source of error is related to the chemical mechanism applied for the modeling of hydrogen oxidation kinetics. Two-dimensional calculations performed beforehand in quiescent conditions have shown that the scatter in lean combustion limit assessed using various schemes of chemical kinetics [44,53–56] comprises 0.10% of hydrogen content in a hydrogen–air mixture or about 2% error relative to the obtained value of the lean combustion limit equal to 5.4% of hydrogen in air. Finally, due to the stochastic nature of the turbulence phenomena, local flow parameters can vary from one calculation to another. However, the integral characteristics of the flow remain almost the same. Additional two-dimensional calculations of the turbulent flame development in a sealed vessel have shown that the maximum pressure realized in the vessel varies in a range $\pm 3\%$ in calculations under the

same process conditions. So, the uncertainties in the lean turbulent limit determination are mainly related to the step of varying the u_{rms} value, while the choice of the chemical kinetic scheme and the local features of the flow field play only a secondary role.

3. Results and Discussion

3.1. Flame Structure in Lean Hydrogen–Air Mixtures

First, let us consider the flame structures of near-limit flames to estimate the governing parameters of lean hydrogen–air combustion. Figure 3a illustrates characteristic temperature and hydrogen concentration profiles in the reaction zone; either it is a deflagration wave or an ultra-lean burning kernel. The fuel is consumed in the reaction zone, as the temperature increases. That straightforward behavior is responsible for the formation of gradients, and exactly those gradients define the flame structure. One can distinguish two basic parameters δ_T and δ_{H_2} characterizing the thermal and diffusion thicknesses of the flame front. As one can clearly see from Figure 3b, at about 11% hydrogen content in the mixture, these spatial scales were equal, while at larger hydrogen content, $\delta_T > \delta_{H_2}$, and at lower hydrogen content, $\delta_T < \delta_{H_2}$. That means the diffusion of mass is dominant compared with the heat transfer in leaner mixtures. At the same time, the key role belongs to the heat transfer in richer mixtures, which is in accordance with the conventional representations of the structure of a deflagration wave. As one can also see from Figure 3c, the role of molecular hydrogen diffusion in the reaction zone propagation increased when the diffusion became dominant over the heat transfer. As soon as the hydrogen content reduced to $\sim 6.5\%$, the normal burning rate was mainly defined by the hydrogen diffusion, which indicated the complete transition to ultra-lean flames [35]. Since there is a transition between the basic mechanisms responsible for hydrogen combustion in the lean region, it is reasonable to use both scales (δ, s_L) when analyzing the effect of turbulence on the combustion. In particular, two Damköhler numbers can be introduced, $Da_T = \frac{\lambda_f s_{L,T}}{\delta_T u_{rms}}$ and $Da_{H_2} = \frac{\lambda_f s_{L,H_2}}{\delta_{H_2} u_{rms}}$. Here, forcing scale λ_f is taken as an integral spatial scale of turbulence and u_{rms} as a pulsation of the velocity in the turbulent field. Currently, it is assumed that $Da > 1$ is the most reasonable criterion for transition from the mode of combustion in the form of separated burning kernels to the mode of flame quenching. Moreover, recently in [32], the calculations via a similar model, although in the case of a closed vessel and integral turbulent scale equal to the size of the vessel, showed that such a criterion was sensible. The criteria for flame quenching by turbulence are considered in the next section.

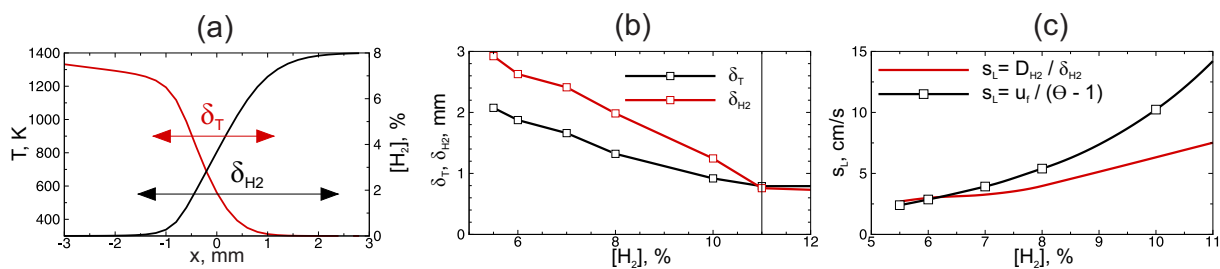


Figure 3. (a) Definition of thermal and diffusion thicknesses in the background of the temperature and hydrogen concentration profiles. (b) Dependence of the thermal and diffusion thicknesses on the hydrogen content in the lean hydrogen–air mixture. (c) Dependence of the characteristic velocity scales on the hydrogen content in the lean hydrogen–air mixture.

3.2. Modes of Flame–Turbulence Interaction and Definition of the Turbulent Combustion Limit

When the flame is affected by turbulence, there are several characteristic modes of turbulent combustion [32]. If the effect of turbulence is weak, the flame is corrugated only by the local vortexes, and with the increase in the turbulence intensity, highly corrugated flames are formed. The existence of highly corrugated flames is conventionally limited with two critical values of the Karlovitz number, Ka_s and Ka_q , from below and above, respectively. Both these values are conditional and are not defined quantitatively. However,

the highly corrugated flame starts breaking up into the separated burning kernels as soon as the turbulence intensity achieves a certain critical value ($Ka \propto Re^{3/2}$). Further intensification of turbulence leads to the mode in which the burning kernels formed in the process of initial flame break up can not maintain combustion, and, finally, each of them quenches, leading to the complete quenching of the combustion.

Figure 4 shows the critical points where the turbulent combustion quenching takes place on the diagram in $(u_{rms}/s_L, \lambda_f/\delta)$ coordinates. Two sets of points calculated for different sets of spatial and velocity scales are shown ($(\delta_T, s_{L,T})$, green signs, and $(\delta_{H_2}, s_{L,H_2})$, red signs). Each point is presented for different hydrogen–air mixtures. The leaner composition corresponds to a larger δ and lower s_L (Figure 3b,c). So the left bottom point corresponds to the 5% hydrogen–air mixture, while the right top point corresponds to the 10% mixture. It is interesting to note that all the points are fitted well by a linear function (both the green and red lines in Figure 4 are linear fits of the corresponding points). So, such a line represents a margin between the combustion in the form of the separated burning kernels and the quenching. The inserts in Figure 4 show characteristic flow patterns in the case of the turbulent combustion development (insert in the right bottom corner) and in the case of the combustion quenching (insert in the left upper corner). Both flow patterns (temperature fields) are shown for the same value of u_{rms} . This demonstrates that the turbulent combustion limit is achieved at a lower turbulence intensity for leaner and less reactive mixtures.

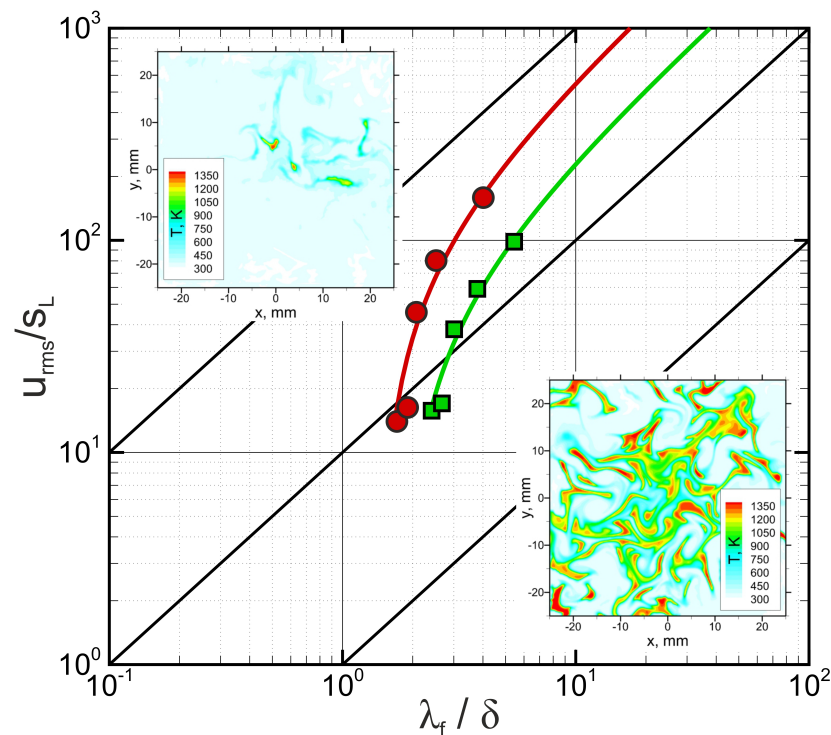


Figure 4. Turbulent combustion limit defined with the use of thermal (green) and diffusion (red) scales for hydrogen–air mixtures containing from 5.5% to 10% of hydrogen content. Points are shown for 5.5%, 6%, 7%, 8%, and 10% hydrogen–air mixtures. The lines are the linear fits. The black lines correspond to $Da = 1, 10,$ and 100 . The inserts show characteristic patterns of the flame kernels in different ranges of turbulence parameters: stable combustion is demonstrated by the example of 10% hydrogen content, $u_{rms} = 5.8$ m/s, quenching mode by 9%, $u_{rms} = 5.8$ m/s.

Conventionally, the turbulent combustion limit is associated with the Damköhler number equal to the unity ($Da = 1$). That is demonstrated by a black line $u_{rms}/s_L = Da \cdot \lambda_f/\delta$ in Figure 4. The lines for $Da = 10$ and $Da = 100$ are presented as well. The criterion found here is also described by a linear law $u_{rms}/s_L = a \cdot \lambda_f/\delta + b$ but with a shift from the center

of coordinates. The coefficient a is estimated as 27.9 when using scales δ_T and $s_{L,T}$ and 63.8 when using scales δ_{H_2} and s_{L,H_2} , which is larger than unity by more than an order.

Let us now compare the obtained estimations for turbulent combustion limits with the known experimental values from the literature. Figure 5 shows the calculated values (black signs) in the background of the experimental data from [14,57,58]. One can see that there is significant scatter in the experimental data. So, it can be concluded that the calculations predict the turbulent combustion limits quite well. Nevertheless, there is a certain underestimation, which can be related to the fact that the characteristics of two-dimensional turbulence are distinct from those of three-dimensional ones. At the same time, however, the obtained results seem to be promising, since even the two-dimensional calculations according to the model proposed in this paper provide acceptable accuracy in the reproduction of different modes of turbulent combustion and in the quantitative assessment of the turbulent combustion limits in lean hydrogen–air mixtures.

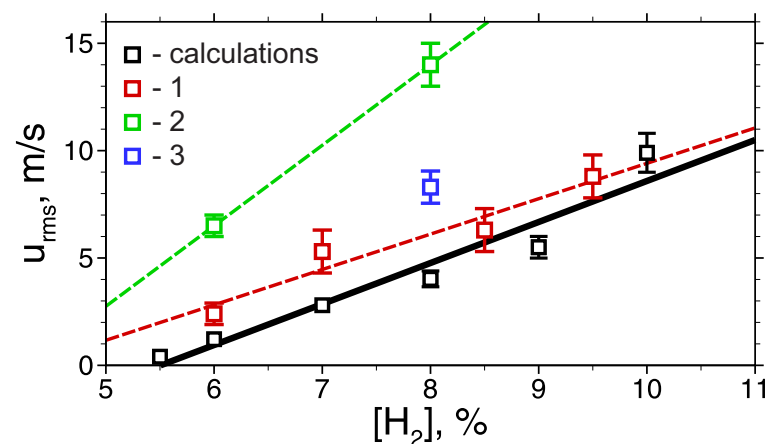


Figure 5. Turbulent combustion limits on the $u_{rms} - [H_2]$ plot compared with three experimental series from [14] (1), [57] (2), and [58] (3).

4. Conclusions

In the present paper, we proposed a numerical model for the estimation of turbulent combustion limits in lean hydrogen–air mixtures that is in demand because of hydrogen safety issues. The proposed model was based on the direct numerical simulation of flame propagation in the synthetically generated turbulent field with given parameters. Here, we provided numerical data for the two-dimensional case of the initially cylindrical flame propagation through the medium where a two-dimensional stationary homogeneous isotropic turbulence was generated beforehand. The obtained numerical data were analyzed, and the turbulent combustion limits were estimated. The obtained values were in good agreement with known experimental data despite the two-dimensional approximation. In view of this, it can be concluded that the proposed approach can be applied for the estimation of turbulent combustion limits in lean hydrogen–air mixtures.

Author Contributions: Conceptualization, A.K. and I.Y.; methodology, A.K., K.M. and I.Y.; software, I.Y.; validation, K.M. and I.Y.; formal analysis, A.K., K.M. and I.Y.; investigation, A.K., K.M. and I.Y.; resources, I.Y.; data curation, K.M. and I.Y.; writing—original draft preparation, I.Y.; writing—review and editing, A.K., K.M. and I.Y.; visualization, A.K., K.M. and I.Y.; supervision, I.Y.; project administration, I.Y.; funding acquisition, I.Y. All authors have read and agreed to the published version of the manuscript.

Funding: I. Yakovenko and K. Melnikova acknowledge the financial support provided by the Grant of the President of Russian Federation for State support of young Russian scientists: [MK-1784.2022.1.1].

Data Availability Statement: The datasets generated and/or analysed during the current study are available from the corresponding author on reasonable request.

Acknowledgments: The authors are grateful to S.P. Medvedev and A.S. Betev for fruitful discussions. The authors acknowledge the high-performance computing support from the Joint Supercomputer Center of the Russian Academy of Sciences.

Conflicts of Interest: The authors declare no conflict of interest.

Abbreviations

The following abbreviations are used in this manuscript:

JANAF Joint Army, Navy, and Air Force

References

1. Coward, H.F.; Jones, G.W. *Limits of Flammability of Gases and Vapors*; Technical Report Bulletin 503; U.S. Bureau of Mines: Washington, DC, USA, 1952.
2. Gelfand, B.E.; Silnikov, M.V.; Medvedev, S.P.; Khomik, S.V. *Thermo-Gas Dynamics of Hydrogen Combustion and Explosion*, 1st ed.; Springer: Berlin/Heidelberg, Germany, 2012.
3. Udagawa, Y.; Yamaguchi, M.; Abe, H.; Sekimura, N.; Fuketa, T. Ab initio study on plane defects in zirconium–hydrogen solid solution and zirconium hydride. *Acta Mater.* **2010**, *58*, 3927–3938. [[CrossRef](#)]
4. Petukhov, V.; Naboko, I.; Fortov, V. Explosion hazard of hydrogen–Air mixtures in the large volumes. *Int. J. Hydrogen Energy* **2009**, *34*, 5924–5931. [[CrossRef](#)]
5. Eichert, H.; Fischer, M. Combustion-related safety aspects of hydrogen in energy applications. *Int. J. Hydrogen Energy* **1986**, *11*, 117–124. [[CrossRef](#)]
6. Kumar, R. Flammability Limits of Hydrogen-Oxygen-Diluent Mixtures. *J. Fire Sci.* **1985**, *3*, 245–262. [[CrossRef](#)]
7. Medvedev, S.P.; Gel'fand, B.E.; Polenov, A.N.; Khomik, S.V. Flammability limits for hydrogen-air mixtures in the presence of ultrafine droplets of water (fog). *Combust. Explos. Shock Waves* **2002**, *38*, 381–386. [[CrossRef](#)]
8. Project SAFEKINEX. *Report on the Experimentally Determined Explosion Limits, Explosion Pressures and Rates of Explosion Pressure Rise*; Technical Report Contractual Deliverable No. 8; Federal Institute for Materials Research and Testing (BAM): Berlin, Germany, 2002.
9. Leblanc, L.; Manoubi, M.; Dennis, K.; Liang, Z.; Radulescu, M.I. Dynamics of unconfined spherical flames. *Phys. Fluids* **2012**, *25*, 091106. [[CrossRef](#)]
10. Ronney, P.D. Near-limit flame structures at low Lewis number. *Combust. Flame* **1990**, *82*, 1–14. [[CrossRef](#)]
11. Yakovenko, I.; Kiverin, A.; Melnikova, K. Ultra-Lean Gaseous Flames in Terrestrial Gravity Conditions. *Fluids* **2021**, *6*, 21. [[CrossRef](#)]
12. Kiverin, A.D.; Yakovenko, I.S.; Melnikova, K.S. On the structure and stability of ultra-lean flames. *J. Phys. Conf. Ser.* **2019**, *1147*, 012048. [[CrossRef](#)]
13. Yang, S.; Saha, A.; Liang, W.; Wu, F.; Law, C.K. Extreme role of preferential diffusion in turbulent flame propagation. *Combust. Flame* **2018**, *188*, 498–504. [[CrossRef](#)]
14. Karpov, V.; Severin, E. Effects of molecular-transport coefficients on the rate of turbulent combustion. *Combust. Explos. Shock Waves* **1980**, *16*, 41–46. [[CrossRef](#)]
15. Abdel-Gayed, R.; Bradley, D. Criteria for turbulent propagation limits of premixed flames. *Combust. Flame* **1985**, *62*, 61–68. [[CrossRef](#)]
16. Chomiak, J.; Jarosiński, J. Flame quenching by turbulence. *Combust. Flame* **1982**, *48*, 241–249. [[CrossRef](#)]
17. Bradley, D.; Shehata, M.; Lawes, M.; Ahmed, P. Flame extinctions: Critical stretch rates and sizes. *Combust. Flame* **2020**, *212*, 459–468. [[CrossRef](#)]
18. Bilger, R.; Pope, S.; Bray, K.; Driscoll, J. Paradigms in turbulent combustion research. *Proc. Combust. Inst.* **2005**, *30*, 21–42. [[CrossRef](#)]
19. Hawkes, E.R.; Sankaran, R.; Sutherland, J.C.; Chen, J.H. Direct numerical simulation of turbulent combustion: Fundamental insights towards predictive models. *J. Phys. Conf. Ser.* **2005**, *16*, 65–79. [[CrossRef](#)]
20. Trisjono, P.; Pitsch, H. Systematic Analysis Strategies for the Development of Combustion Models from DNS: A Review. *Flow Turbul. Combust.* **2015**, *95*, 231–259. [[CrossRef](#)]
21. Williams, F.A. *Combustion Theory*, 2nd ed.; CRC Press: Boca Raton, FL, USA, 1985.
22. Cant, R.; Pope, S.; Bray, K. Modelling of flamelet surface-to-volume ratio in turbulent premixed combustion. *Symp. Int. Combust.* **1991**, *23*, 809–815. [[CrossRef](#)]
23. Bechtold, J.K.; Matalon, M. The dependence of the Markstein length on stoichiometry. *Combust. Flame* **2001**, *127*, 1906–1913. [[CrossRef](#)]
24. Giannakopoulos, G.K.; Gatzoulis, A.; Frouzakis, C.E.; Matalon, M.; Tomboulides, A.G. Consistent definitions of “Flame Displacement Speed” and “Markstein Length” for premixed flame propagation. *Combust. Flame* **2015**, *162*, 1249–1264. [[CrossRef](#)]
25. Dave, H.L.; Chaudhuri, S. Evolution of local flame displacement speeds in turbulence. *J. Fluid Mech.* **2020**, *884*, A46. [[CrossRef](#)]

26. Lipatnikov, A.; Nishiki, S.; Hasegawa, T. Closure Relations for Fluxes of Flame Surface Density and Scalar Dissipation Rate in Turbulent Premixed Flames. *Fluids* **2019**, *4*, 43. [[CrossRef](#)]
27. Pope, S.B. PDF methods for turbulent reactive flows. *Prog. Energy Combust. Sci.* **1985**, *11*, 119–192. [[CrossRef](#)]
28. Kuznetsov, V.R.; Sabelnikov, V.A. *Turbulence and Combustion*, 1st ed.; Hemisphere Publishing Corporation: New York, NY, USA, 1990.
29. Haworth, D.C. Progress in probability density function methods for turbulent reacting flows. *Prog. Energy Combust. Sci.* **2010**, *36*, 168–259. [[CrossRef](#)]
30. Zimont, V.L. Conceptual Limitations of the Probability Density Function Method for Modeling Turbulent Premixed Combustion and Closed-Form Description of Chemical Reactions' Effects. *Fluids* **2021**, *6*, 142. [[CrossRef](#)]
31. Sabelnikov, V.A.; Lipatnikov, A.N. A new mathematical framework for describing thin-reaction-zone regime of turbulent reacting flows at low damköhler number. *Fluids* **2020**, *5*, 109. [[CrossRef](#)]
32. Betev, A.; Kiverin, A.; Medvedev, S.; Yakovenko, I. Numerical Simulation of Turbulent Hydrogen Combustion Regimes Near the Lean Limit. *Russ. J. Phys. Chem. B* **2020**, *14*, 940–945. [[CrossRef](#)]
33. Uranakara, H.A.; Chaudhuri, S.; Lakshmisha, K. On the extinction of igniting kernels in near-isotropic turbulence. *Proc. Combust. Inst.* **2017**, *36*, 1793–1800. [[CrossRef](#)]
34. Volodin, V.V.; Golub, V.V.; Kiverin, A.D.; Melnikova, K.S.; Mikushkin, A.Y.; Yakovenko, I.S. Large-scale Dynamics of Ultra-lean Hydrogen-air Flame Kernels in Terrestrial Gravity Conditions. *Combust. Sci. Technol.* **2020**, *193*, 225–234. [[CrossRef](#)]
35. Yakovenko, I.S.; Ivanov, M.F.; Kiverin, A.D.; Melnikova, K.S. Large-scale flame structures in ultra-lean hydrogen-air mixtures. *Int. J. Hydrogen Energy* **2018**, *43*, 1894–1901. [[CrossRef](#)]
36. Ronney, P.D.; Whaling, K.N.; Abbud-Madrid, A.; Gatto, J.L.; Pisowicz, V.L. Stationary premixed flames in spherical and cylindrical geometries. *AIAA J.* **1994**, *32*, 569–577. [[CrossRef](#)]
37. Kuo, K.K.; Acharya, R. *Fundamentals of Turbulent and Multiphase Combustion*, 1st ed.; John Wiley & Sons, Inc.: Hoboken, NJ, USA, 2012.
38. Poinot, T.; Veynante, D. *Theoretical Numerical Combustion*, 2nd ed.; R.T. Edwards, Inc.: Philadelphia, PA, USA, 2005.
39. Bykov, V.; Kiverin, A.; Koksharov, A.; Yakovenko, I. Analysis of transient combustion with the use of contemporary CFD techniques. *Comput. Fluids* **2019**, *194*, 104310. [[CrossRef](#)]
40. Chase, M.W. *NIST-JANAF Thermochemical Tables*, 4th ed.; American Institute of Physics: Woodbury, NY, USA, 1998; Volume 9.
41. Hirschfelder, J.O.; Curtiss, C.F.; Bird, R.B. *The Molecular Theory of Gases and Liquids*, Revised ed.; Wiley-Interscience: Hoboken, NJ, USA, 1964.
42. Kee, R.J.; Coltrin, M.E.; Glarborg, P. *Chemically Reacting Flow: Theory and Practice*, 1st ed.; Wiley-Interscience: Hoboken, NJ, USA, 2003.
43. Coffee, T.; Heimerl, J. Transport algorithms for premixed, laminar steady-state flames. *Combust. Flame* **1981**, *43*, 273–289. [[CrossRef](#)]
44. Kéromnès, A.; Metcalfe, W.K.; Heufer, K.A.; Donohoe, N.; Das, A.K.; Sung, C.J.; Herzler, J.; Naumann, C.; Griebel, P.; Mathieu, O.; et al. An experimental and detailed chemical kinetic modeling study of hydrogen and syngas mixture oxidation at elevated pressures. *Combust. Flame* **2013**, *160*, 995–1011. [[CrossRef](#)]
45. McGrattan, K.; McDermott, R.; Hostikka, S.; Floyd, J.; Vanella, M. *Fire Dynamics Simulator Technical Reference Guide Volume 1: Mathematical Model*; Technical Report NIST Special Publication 1018-1; U.S. Department of Commerce, National Institute of Standards and Technology: Gaithersburg, MD, USA, 2019. [[CrossRef](#)]
46. Carroll, P.L.; Blanquart, G. A proposed modification to Lundgren's physical space velocity forcing method for isotropic turbulence. *Phys. Fluids* **2013**, *25*, 105114. [[CrossRef](#)]
47. Lu, Z.; Yang, Y. Modeling pressure effects on the turbulent burning velocity for lean hydrogen/air premixed combustion. *Proc. Combust. Inst.* **2021**, *38*, 2901–2908. [[CrossRef](#)]
48. Wang, Z.; Abraham, J. Effects of Karlovitz Number on Flame Surface Wrinkling in Turbulent Lean Premixed Methane-Air Flames. *Combust. Sci. Technol.* **2018**, *190*, 363–392. [[CrossRef](#)]
49. Basevich, V.Y.; Belyaev, A.A.; Frolov, S.M.; Frolov, F.S. Direct Numerical Simulation of Turbulent Combustion of Hydrogen—Air Mixtures of Various Compositions in a Two-Dimensional Approximation. *Russ. J. Phys. Chem. B* **2019**, *13*, 75–85. [[CrossRef](#)]
50. Haugen, N.E.L.; Brandenburg, A.; Dobler, W. Simulations of nonhelical hydromagnetic turbulence. *Phys. Rev. E Stat. Phys. Plasmas Fluids Relat. Interdiscip. Top.* **2004**, *70*, 14. [[CrossRef](#)]
51. Semenov, E.S. Measurement of turbulence characteristics in a closed volume with artificial turbulence. *Combust. Explos. Shock Waves* **1965**, *1*, 57–62. [[CrossRef](#)]
52. Karpov, V.P.; Semenov, E.S.; Sokolik, A.S. Turbulent combustion in closed volume. *Dokl. USSR* **1959**, *128*, 1220–1223.
53. Kusharin, A.Y.; Agafonov, G.L.; Popov, O.E.; Gelfand, B.E. Detonability of H₂/CO/CO₂/Air Mixtures. *Combust. Sci. Technol.* **1998**, *135*, 85–98. [[CrossRef](#)]
54. Konnov, A. Refinement of the kinetic mechanism of hydrogen combustion. *Khimicheskaya Fiz.* **2004**, *23*, 5–19.
55. Boivin, P. Reduced-Kinetic Mechanisms for Hydrogen and Syngas Combustion Including Autoignition. Ph.D. Thesis, Universidad Carlos III de Madrid, Leganés, Spain, 2011.
56. Starik, A.; Titova, N. Kinetics of detonation initiation in the supersonic flow of the H₂ + O₂ (air) mixture in O₂ molecule excitation by resonance laser radiation. *Kinet. Catal.* **2003**, *44*, 28–39. [[CrossRef](#)]

-
57. Al-Khishali, K.; Bradley, D.; Hall, S. Turbulent combustion of near-limit hydrogen-air mixtures. *Combust. Flame* **1983**, *54*, 61–70. [[CrossRef](#)]
 58. Breitung, W.; Chan, C.; Dorofeev, S.; Eder, A.; Gelfand, B.; Heitch, M.; Klein, R.; Malliakos, A.; Shepherd, J.; Studer, A.; et al. *Flame Acceleration and Deflagration-to-Detonation Transition in Nuclear Safety, State-of-the-Art Report by a Group of Experts*; Technical Report; Technical Report No. NEA/CSNI; OECD Nuclear Energy Agency: Le Seine Saint-Germain, France, 2000.